

# SFSA Cast In Steel 2026 – Horsemans Axe Technical Report

Wentworth Inst. Of Technology: 31in. of OSHA Non-Compliance



### Team Members:

Jacob Forrette (Leader), Josh Hofer, , Robert Stewart, Luis Leins, Brady McDonald

### Faculty Advisor:

Serdar Tumkor, Ph.D.

Associate Professor, William E. Roberts Professor, FEF Key Professor

### Sponsor Foundry:



## Executive Summary

The Steel Founders' Society of America (SFSA) Cast in Steel competition challenges student teams to design and manufacture functional steel components using modern casting technology. For the 2026 competition, teams had to produce a historically inspired Horseman's Axe that demonstrates sound engineering, effective casting, and validated structural integrity through inspection and testing [1].

Steel casting introduces unique challenges, including small holes in the metal from shrinking (shrinkage porosity), control over how the metal hardens (directional solidification), and the way the molten metal moves into the mold (mold-filling behavior). The axe head was intentionally designed with these principles in mind, using computer modeling (simulation) and improved flow pathways (gating optimization) to ensure strength and ease of manufacturing.

The Wentworth Institute of Technology team designed and produced a Horseman's Axe using CA6NM martensitic stainless steel and a chemically bonded, no-bake sand-casting process with 3D-printed molds. The design prioritized castability, structural integrity, and historical authenticity while maintaining the competition's weight and size constraints.

Computer simulation software called MAGMASoft was used to predict how the molten metal would flow into the mold, how it would solidify, and where any defects might form before actual casting. The simulation results were used to fine-tune the molten steel's entry into the mold, ensuring the metal moved in the right direction and solidified without forming unwanted gaps or shrinkage-related weak spots.

Following casting, the axe head underwent machining, heat treatment, inspection, and testing. Non-destructive testing methods, including visual inspection, liquid penetrant testing, and ultrasonic testing, were used to verify structural integrity. Mechanical evaluation included hardness testing and Charpy V-notch impact testing, while physical testing evaluated cutting performance and durability.

The final axe demonstrated satisfactory structural integrity and maintained cutting performance during repeated impact testing. The final axe measured **30.75 inches** in length and **weighed 2.78 lb**, meeting the competition requirements for size and weight; the final dimensions and test results are summarized in **Table A1**.

## Historical Background

Horseman's axes were used by mounted warriors from the 14th to 17th centuries and were designed to be compact, versatile, and controllable with one hand. They typically featured a curved blade for slicing and a rear spike for penetrating armor.

The Wentworth design was inspired by a historical example from the Art Institute of Chicago and adapted for modern steel casting while preserving the weapon's broad blade, rear spike, and reinforced handle socket, as shown in **Figure A1** [2].

## **Design Methodology**

The design emphasized a clean, functional form, easy to manufacture and inspect. Sharp transitions and complexity were reduced to lower stress and defects. Material was added for strength and balance, while non-critical material was removed to stay within the 1.5 kg (3.3 lb) limit.

### **Material & Casting Selection:**

CA6NM martensitic stainless steel was selected for the Horseman's Axe because it provides a strong combination of strength, toughness, corrosion resistance, and castability. The axe head was produced using chemically bonded no-bake sand casting with 3D-printed sand molds, which supported the part's complex geometry and allowed rapid design iteration without permanent tooling, as represented by the mold design shown in **Figure A4**.

### **Material Properties:**

CA6NM is a low-carbon, 12–13% chromium martensitic stainless steel with nickel and molybdenum additions to enhance toughness and corrosion resistance. The nominal chemical composition includes approximately 11.5–14% chromium, 3.5–4.5% nickel, 0.4–1.0% molybdenum, and a maximum carbon content of 0.06% [3]

Typical mechanical properties after proper heat treatment include:

- Ultimate tensile strength: ~100–120 ksi
- Yield strength: ~70–90 ksi
- Elongation: ~15–20%
- Hardness: approximately 250–300 HB (depending on tempering condition)
- Charpy V-notch impact toughness: typically in the range of 20–40 ft-lb at room temperature)

These properties provide a favorable balance between hardness for edge retention and toughness for impact resistance.

### **Design of the Axe Handle:**

The handle is made of American Black Hickory wood and has a smooth, rounded, ergonomic form. It features a subtle taper, a gentle lower curve. Keeping a slightly flared butt with a rounded knob prevents slipping during use. The head of the handle is designed to fit the oval-shaped pocket machined into the

axe head. The interface between the handle and axe head was developed to provide a secure fit and resist twisting during impact, as reflected in the modeled geometry shown in **Figure A3**.

## **Casting and Fabrication**

### **Sponsor Foundry**

D.W. Clark was selected as the foundry partner for this project due to its expertise in advanced casting processes and precision manufacturing [4]. Located in Taunton, Massachusetts, the company specializes in engineered sand casting and centrifugal casting for defense, marine, energy, and industrial manufacturing industries. The foundry also utilizes 3D-printed sand molds, enabling complex geometries and precision comparable to investment casting while reducing tooling costs. In addition to casting support, D.W. Clark collaborated with the team during machining and inspection of the axe heads and provided access to a CNC 3-axis mill and non-destructive testing equipment. This partnership offered valuable exposure to real-world casting, metallurgy, and industrial production practices.

### **Engineering Design and Model Development**

The engineering process began with a 3D CAD model developed in Onshape, shown in **Figure A3**. Later iterations focused on improving castability and manufacturability by reducing areas prone to shrinkage and incomplete filling. Fillets were added to reduce stress concentrations and improve metal flow during solidification. Extra machining stock was included where needed, and the handle pocket region was refined to improve filling and final strength. The spike and blade geometry were also slightly thickened relative to the historical reference to improve durability during impact testing. Material was removed from non-critical areas to maintain the competition weight limit while preserving strength in high-stress regions.

### **Solidification and Process Simulation**

Solidification and process simulations were conducted using MAGMAsoft to evaluate casting behavior prior to physical production. Initial “naked” simulations, consisting solely of the casting geometry without rigging, were performed to establish a theoretical baseline for solidification behavior. These simulations were used to identify thermal gradients, solidification paths, and potential hot spots. Predicted porosity from the initial simulation is shown in **Figure A2**, while predicted microporosity is shown in **Figure A6**. After the rigging concepts were developed, additional simulation runs were performed to evaluate directional solidification and liquid-metal behavior throughout the casting process, as illustrated in **Figure A5**.

Based on these results, layout planning and risk analysis were conducted to compare direct-pour and conventionally gated configurations. Rigging systems, including risers and gas vents, were then designed to promote directional solidification and facilitate gas evacuation. A direct-pour configuration incorporating gas vents along the blade region was selected and evaluated through additional MAGMASoft simulations to assess overall process viability. The solidification behavior is illustrated in **Figure A5**.

### **Simulation Analysis and Gating Development**

Simulation results were analyzed to identify predicted porosity, hot spots, and metal flow behavior, as shown in **Figures A2, A5, and A6**. Based on these findings, the gating design was refined by relocating the direct-pour position above the handle pocket to improve filling and feeding in that critical region. Temperature and filling time were calculated using a target temperature range of 2950–3050 °F, with filling time estimated using a square-root relationship relative to total pour weight.

### **Verification of Filling Parameters**

The filling simulations showed that the metal temperature stayed above the point where it remains liquid throughout the mold-filling stage. The metal's speed as it filled the mold remained below 20 inches per second, which helps prevent swirling and air entrapment that can cause defects, as shown in **Figure A7**.

### **Final Design Review and Mold Preparation**

A final design review was conducted to evaluate the venting strategy, mold coating selection, and a comprehensive risk assessment addressing all identified failure modes. Upon approval, a complete three-dimensional mold assembly was generated and submitted for fabrication via sand 3D printing, as shown in **Figure A4**. Following printing, the mold components were assembled and prepared for pouring.

### **Pouring and Solidification**

During the pouring operation, the molten metal's chemical composition was verified by optical emission spectroscopy to ensure compliance with the specified alloy requirements. The measured composition closely matched the target CA6NM corrosion-resistant martensitic stainless steel chemistry. This confirms that the melt chemistry met the requirements for CA6NM cast steel as defined by the Steel Founders' Society of America [3]. These pouring conditions were selected to align with the predicted filling and solidification behavior observed in **Figure A5**.

The tap temperature at the time of pouring was **3016 °F**, which exceeds the nominal melting temperature of approximately **2750 °F** for CA6NM and provided sufficient superheat to ensure adequate fluidity and complete mold filling [3]

The casting was poured in **3.47 s**, producing a measured pour weight of **3.64 lb**. These parameters were selected to balance flow stability, minimize turbulence, and promote sound solidification. Following completion of the pour, the casting was allowed to cool and solidify under controlled conditions prior to removal from the mold.

The casting yield was evaluated to understand the efficiency of the gating system. The casting yield was approximately 86%, calculated from a final axe head weight of 3.14 lb and a total pour weight of 3.64 lb. The direct-pour configuration minimized the amount of gating material required while maintaining adequate feeding during solidification. This approach improved casting efficiency while maintaining acceptable defect control. The selected pouring parameters were consistent with the simulated solidification behavior shown in **Figure A5**.

### **Final Machining**

Following mechanical verification, final machining operations were performed. Custom soft jaws were designed, CNC-programmed, and machined to precisely locate and constrain the casting while ensuring secure clamping loads. CNC machining programs were then developed for the handle pocket and blade contour features.

After CNC machining, the team used an angle grinder and sandpaper to achieve a clean finish on the heads. Before this, we used a manual mill to drill a 3/16" hole in the head for the rivets that hold the straps and handle together. Additionally, a polisher was used to achieve a mirror finish from the rough-sanded state.

### **Heat Treatment**

Heat treatment was performed as specified in **Table A2**. The initial heat treat process used a three step method consisting of an annealing cycle and austenizing cycle to reduce residual stress and homogenize grain structure increasing durability and reducing the risk of chipping and cracking in the axe head. The final step was a full body oil quench of the axe at critical temperature to get a consistent and hard martensitic grain structure for strength and edge retention. The first three steps were courtesy of D.W. Clark and run with other parts for fuel conservation. Unfortunately the rapid cooling and larger thermal mass of the blade resulted in cracking around the base of the blade due to stress from thermal

shock as simulated in **figure A12** and shown in **figure A13**. Because of this, the cracks were ground out and GTAW welded with ER410NiMo and appropriate preheat, interpass temperatures, and post heat. Due to the high martensitic properties and localized heating an additional austenizing cycle was run to reduce stress and homogenize the heat affected zone to eliminate any stress. After that a temper was used to further reduce stress in the body of the blade since the austenizing was conducted in 18 degree fahrenheit ambient conditions and despite insulation, cooled faster than anticipated. The final heat treatment cycle was an edge quench to increase hardness on the cutting edge of the blade.

## **Handle Fabrication**

The handle was manufactured from American black hickory, selected for its high impact strength, shock resistance, and favorable grain structure for load and impact bearing. Grain orientation was carefully selected to ensure the fibers ran along the primary load axis, improving fatigue resistance and reducing the risk of cracking.

The stock was cut into blanks measuring 2.0 in  $\times$  3.125 in  $\times$  27.0 in, and a full-scale template was used to establish the ergonomic profile and maintain dimensional consistency. The rough shape was cut using a bandsaw, leaving excess material for refinement. Final shaping was completed with a flap disk and belt sander to achieve the desired contour with a hand-sanded surface finish. Multiple coats of linseed oil were applied to provide moisture resistance, reduce surface checking, and improve long-term durability while preserving the wood's natural properties. The surface was also lightly burnt for aesthetic reasons.

## **Technical Specifications:**

The team's axe is modeled after horsemen's axes used by mounted soldiers between the 14th and 17th centuries, when cavalry required weapons that were compact, fast, and controllable with one hand while managing the reins. The mid-length shaft and balanced proportions reflect this need for mobility and leverage from horseback. Its broad cutting blade is designed for powerful slicing strikes, while the rear spike represents the armor-piercing features commonly found on cavalry axes used against mail or gaps in plate armor. Together, the blade, spike, and reinforced head construction reflect the versatility and practicality typical of historical horsemen's axes [5]. These features are consistent with the historical reference shown in **Figure A1** and the modeled geometry shown in **Figure A3**.

## **Axe Dimensions**

The final axe dimensions are summarized in **Table A1**, while the overall geometry is shown in **Figure A3**.

## Proportion and balance

The proportions were selected to preserve historical form while maintaining balance and usability, as reflected in **Figure A3**.

## Features and Design

Key design features, including the broad blade, rear spike, and reinforced socket region, are visible in **Figures A1 and A3**.

## Testing Analysis

### Comparative analysis

Finite element analysis was performed using SolidWorks Simulation to evaluate the structural response of the axe head under loading, as shown in Figures A8–A10. A 500 lbf load was applied to the blade region to estimate deformation and stress distribution under severe service conditions. The predicted maximum deformation was less than 0.0007 in (Figure A8), while additional edge-loading and stress plots (Figures A9 and A10) showed that the highest stresses were concentrated near geometric transitions and loaded regions. These results suggested that the axe head would remain structurally stable under the applied load and supported the final geometry prior to fabrication.

### Hardness testing

Hardness testing was performed to verify the effectiveness of the heat treatment process. A sample was taken by cutting the riser from the casting, then the surface was ground to a smooth finish and polished to ensure accurate, consistent test results. Once calibrated, the sample was tested, and the measured hardness was approximately 384 Brinell. This result indicates that the heat treatment produced a hardened microstructure consistent with the expected mechanical properties for the material.

### Charpy V Notch Impact Testing

Macroscopic examination of the Charpy V-notch fracture surfaces revealed differences in internal soundness and fracture behavior between the two specimens, shown in **Figure A11**. Sample 1 exhibited a central cavity at the fracture surface consistent with gas porosity or entrapped air introduced during casting. This defect likely acted as a stress concentrator, influencing crack initiation and fracture propagation during impact loading. Sample 2 displayed a uniform fracture surface with no visible macroscopic defects, indicating improved internal soundness and more uniform solidification. Sample 1 absorbed a higher impact energy (33.33 ft-lb) than Sample 2 (29.83 ft-lb); however, this increase is attributed to defect-driven fracture behavior rather than improved intrinsic material toughness. Sample 2,

therefore, provides a more representative measure of the material's impact performance due to its cleaner fracture surface and absence of significant casting defects.

### **NDT testing**

Liquid penetrant testing was then used to define the extent of the surface defects. Initial heat treatment had resulted in a crack that had propagated around the larger blade section of the axe head, as shown in Figure A13. After consultation with the sponsor foundry, a weld repair was performed to restore structural continuity. The casting was then subjected to repeated visual inspection, liquid penetrant testing, and ultrasonic testing, which confirmed that the repair restored structural integrity and that no remaining defects were detected. Following this, a second heat-treatment cycle was used to restore mechanical properties after the thermal shock induced by the welding repair shown in Table A2.

### **Physical testing**

Physical testing was performed to evaluate cutting performance, edge durability, and structural integrity under simulated service conditions. The axe was repeatedly struck into solid wood to assess edge retention and handle stability. Additional impacts against thin sheet metal were used to evaluate toughness and resistance to chipping or deformation. After testing, the axe showed no cracks, edge failure, or handle loosening, and it maintained its cutting ability.

Overall, fracture analysis, non-destructive testing, and physical performance tests confirmed that the cast axe head achieved acceptable structural integrity when free of significant casting defects. Although Charpy testing showed that internal defects could affect impact energy, NDT successfully identified and verified repaired areas. Final physical testing confirmed the effectiveness of these repairs, demonstrating that the axe maintained edge integrity, toughness, and handle stability under repeated loading, indicating the casting and post-processing methods produced a durable and functional component.

### **Casting Challenges and Solutions**

A crack formed around the blade during heat treatment, which is consistent with the stress concentration pattern predicted in **Figure A12**. Following the final heat treatment, the axe head was full-body oil-quenched, resulting in a stress riser where the thin blade met the higher thermal volume of the body. Non-destructive testing identified the extent of the defect, and the component was successfully repaired using weld repair followed by re-heat treatment, as shown in **Table A2**. Subsequent ultrasonic and penetrant testing confirmed that the repair restored structural integrity.

The repair and verification process confirmed that industry-standard weld repair techniques can restore structural integrity in high-alloy cast steel components when properly controlled.

## **Conclusion and Recommendations**

The SFSA Cast in Steel 2026 Horseman's Axe project met the competition requirements for design, manufacturing, and verification. Using CA6NM stainless steel, MAGMASoft simulation, and controlled casting methods, the team produced a functional and historically inspired axe that met the required size, weight, and material constraints. Inspection and testing, including Charpy impact testing, non-destructive testing, and physical performance trials, confirmed the axe's structural integrity, durability, and cutting performance. The integration of casting simulation, careful gating design, and rigorous inspection procedures allowed the team to control casting defects and achieve a structurally sound final product. Overall, the project demonstrated that modern steel-casting methods can successfully produce a durable, high-performance historical weapon.

## **References:**

- [1] Cast in Steel, "Cast in Steel 2026 – Horseman's Axe." Accessed: Aug. 10, 2025
- [2] Art Institute of Chicago, "Horseman's axe," artwork page. Accessed: Aug. 20, 2025.
- [3] Steel Founders' Society of America, *Steel Castings Handbook: Supplement 8 – High Alloy Data Sheets, Corrosion Series*, 2004.
- [4] D.W. Clark, "Precision Sand Castings," 2025. Accessed: Sept. 15, 2025.
- [5] Warfare History Network, "The Battle-Ax," Warfare History Network. Accessed: 3/01/2026

## Acknowledgements:

The team would like to express sincere gratitude to **Wentworth Institute of Technology** for providing the education, facilities, and academic foundation that made this project possible. The knowledge gained through coursework, design work, and technical analysis was instrumental throughout all phases of development. We are especially thankful for the institutional support that enabled hands-on learning and industry collaboration.

We extend our appreciation to **D.W. Clark** for their generous sponsorship, technical expertise, and access to advanced casting, machining, and inspection resources. In particular, we thank **Josh R.** for his engineering insight and mold-making expertise, which were critical to achieving a successful casting. We are also grateful to **Kevin R** for his exceptional machining skills and attention to detail in shaping the axe head and associated components, ensuring dimensional accuracy, balance, and overall quality.

The team would also like to thank **Readers Hardwood** for generously donating the wood used in the handle, which contributed significantly to the final assembly. Additional appreciation is extended to the **American Foundry Society, particularly the New England Chapter**, for its continued support of student involvement in the steel-casting community. A special thank you is given to **Will Shambley** for his fundraising assistance and valuable guidance throughout the competition.

Finally, we gratefully acknowledge the **Steel Founders' Society of America** for organizing the Cast in Steel competition. This event provided an invaluable opportunity to apply engineering principles in a real-world context while fostering innovation, craftsmanship, and professional growth.

## Appendix A. Figures and Tables



**Caption A1:** Visual Inspiration from Art Institute of Chicago of Horseman's Axe [2]

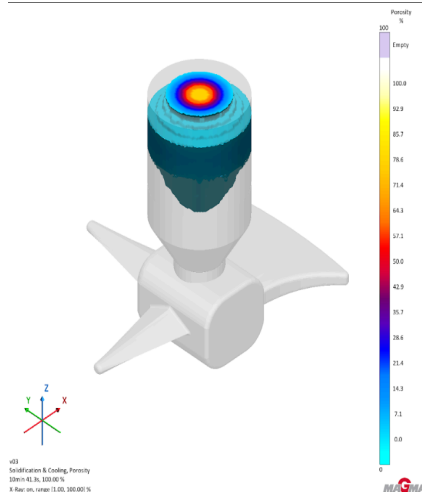


**Figure A2.** Solidification and cooling simulation showing predicted porosity

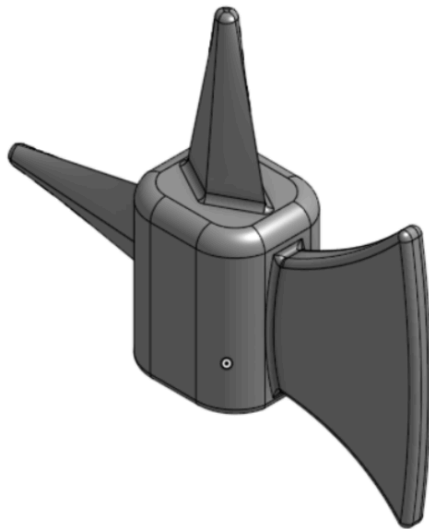


**Figure A3.** Onshape 3D model of the axe

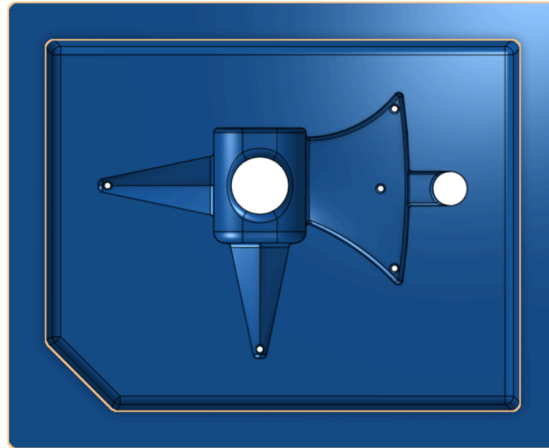


**Figure A4.** Onshape 3D model of the sand mold

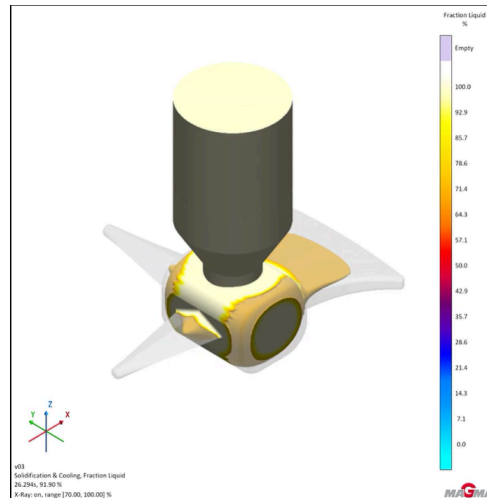


**Figure A5.** Solidification & Cooling, Fraction Liquid

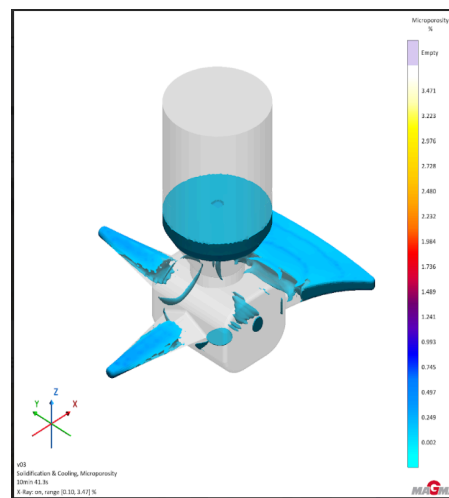


**Figure A6.** Solidification and cooling simulation showing predicted microporosity

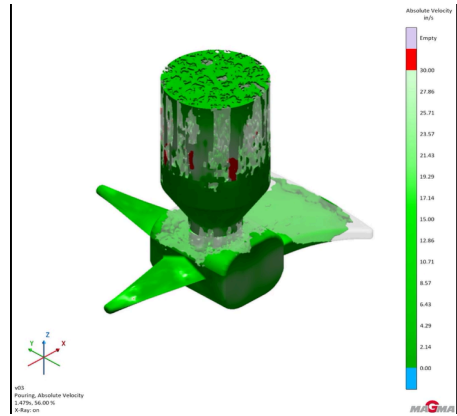


Figure A7. Simulation of Pouring Velocity

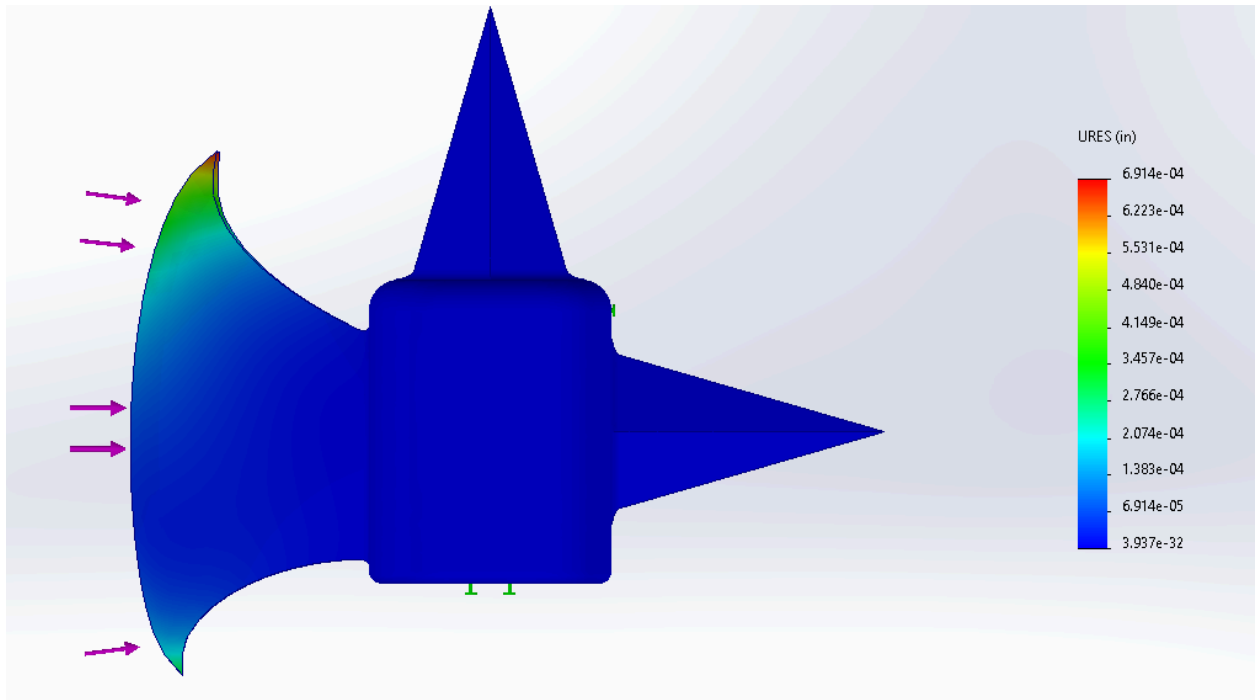


Figure A8. SolidWorks simulation of the axe head under a 500 lbf load

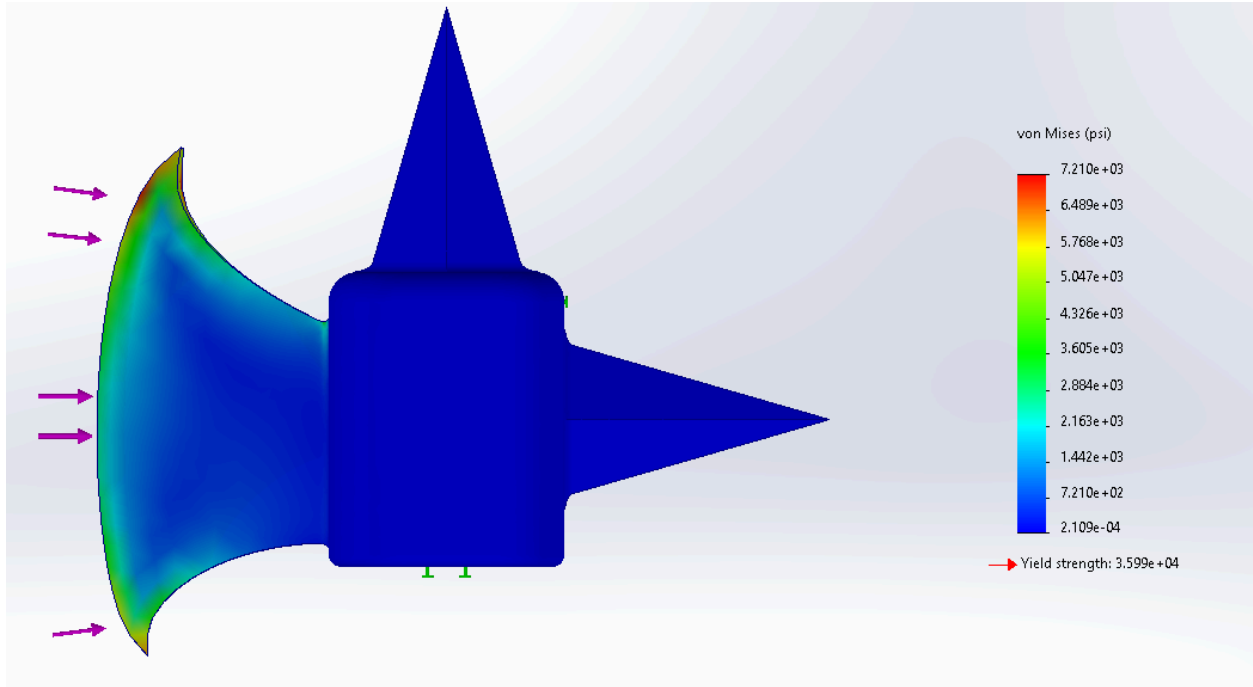
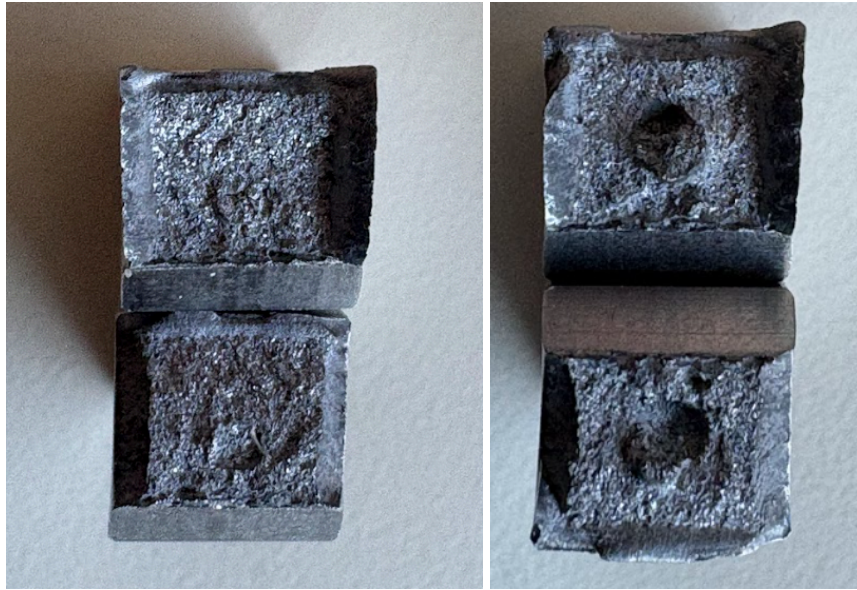


Figure A9: Simulation 2 of load on the whole Edge

Study name	Static 1* (-Default-)
DetailsMesh type	Solid Mesh
Mesher Used	Blended curvature-based mesh
Jacobian points for High quality mesh	16 points
Max Element Size	9.31156 mm
Min Element Size	0.972016 mm
Mesh quality	High
Total nodes	28878
Total elements	17479
Maximum Aspect Ratio	19.457
Percentage of elements with Aspect Ratio < 3	92.4
Percentage of elements with Aspect Ratio > 10	0.137
Percentage of distorted elements	0
Number of distorted elements	0
Reuse mesh for identical bodies	Off
Number of bodies that have reused mesh	0
Time to complete mesh(hh:mm:ss)	00:00:05
Computer name	

Figure A10: FEA Results



**Figure A11.** Charpy test specimens after fracture

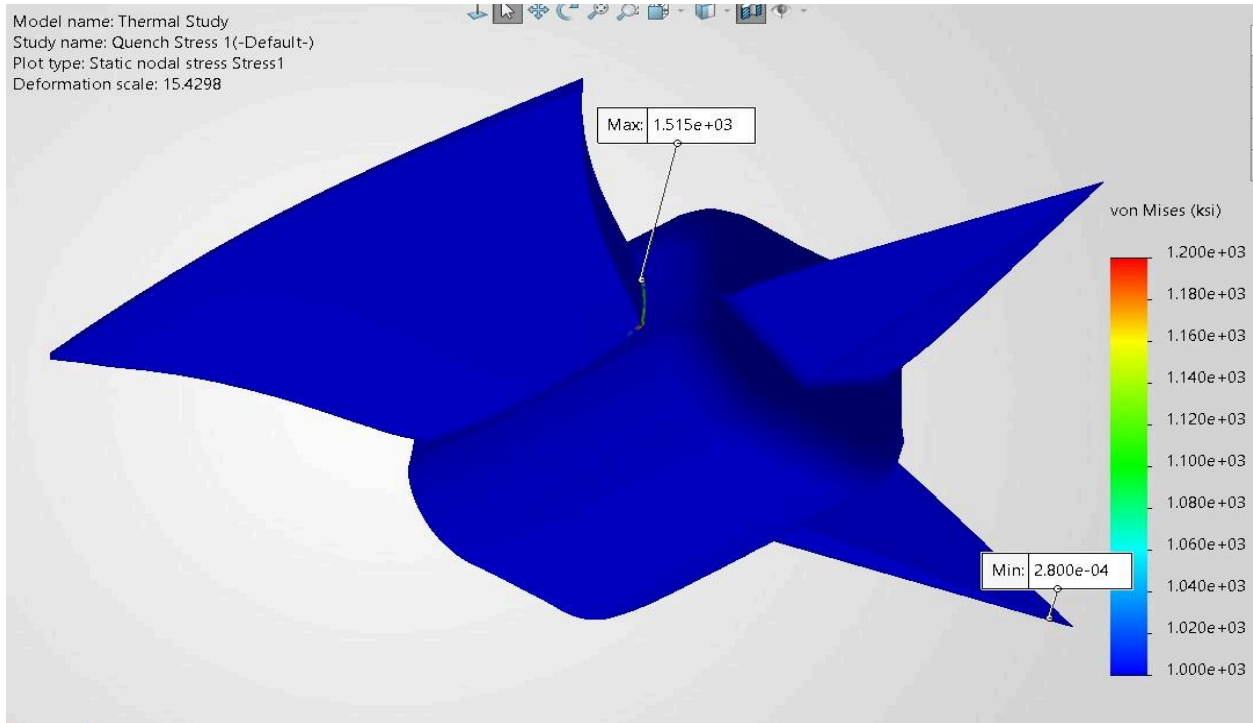


**Figure A12.** Simulation of Stress Concentration During Quench



**Figure A13.** Axe head after liquid penetrant testing

<b>Property</b>	<b>Values</b>
Overall Length	30.75 in
Total Weight	2.87 lbs
Machined Head Weight	2.78
Blade Length along the Curve	3.699
Blade Thickness at base	.514
Blade Thickness at bevel	.172
Spike thickness at Base	.581
Spike width at base	1.245
Wall Thickness of Head	.278 min
Handle Length	25 5/8
Handle Width	1.84 max, 1.152 min
Strap length	4
Strap Width	.991
Rivet Dimensions	3/16 in Dimeter
Hardness	384 Brinell
Charpy Impact	31.13 ft-lb

**Table A1.** Final measurements and test results for the Horseman's Axe

<b>Cycle</b>	<b>Temp (F)</b>	<b>Soak Time (min)</b>
Annealing 1 (First of two annealing cycles to homogenize grain/reduce stress)	1850	420
Annealing 2 (Austenizing cycle to homogenize grain/reduce stress, then air harden non-cutting edges)	1250	405
Heat Treatment 3 (Final heat to quenching temperature)	1150	360
Full Body Quench (Full body oil quench for strength and increased hardness)	1150	N/A
Initial Anneal (to reduce residual stress from quenching before gouging of the part)	1885	30
Welding Repair Preheat (to reduce thermal shock during welding and expel moisture)	212-338	N/A
Welding Max Interpass Temp (To ensure consistency in weld mechanical properties)	599	N/A
Austenizing (To reduce residual stress in the heat-affected zone of the weld, homogenize, and increase toughness)	1880	52
Final Temper (To reduce hardness and improve plasticity and durability under impact)	1035	26
Edge Quench (To increase hardness at the cutting edge while inducing less stress on the rest of the part)	1872	N/A

**Table A2.** Heat Treatment Parameters and Cycles